



## Influence of Die Geometry on the Joint Interlock of Aluminum Sheets Using Self-Piercing Rivet

Haibat Lafta<sup>1\*</sup> and Doaa Fadil Mohammed<sup>2</sup>

<sup>1</sup> Middle Technical University

<sup>2</sup> Al-Qasim green University

*Corresponding Author Email: [haibat-lafta@mtu.edu.iq](mailto:haibat-lafta@mtu.edu.iq)*

Received Jul.18, 2025

Revised Oct.9, 2025

Accepted Dec.23, 2025

Online March.1, 2026

### ABSTRACT

This study investigates how die geometry affects joint interlock in aluminum sheets of variable thickness joined by self-piercing riveting (SPR). Lap shear and T-peel tests were conducted to evaluate the effects of die configurations and sheet thickness on joint quality. Joint interlock, rivet head height, and minimum remaining material thickness were measured experimentally under a constant riveting load of 17 kN. Three sets of similar sheet combinations (0.9+0.9 mm, 0.7+0.7 mm, and 0.5+0.5 mm) and different thickness distributions (e.g., 0.5+0.7 mm, 0.5+0.9 mm, and 0.9+0.7 mm) were tested using twelve different die configurations. A finite element model was established to forecast the flow of material in rivets, and a neural network approach was implemented to analyze the combined experimental and simulated results. The findings show that joint interlock increased with sheet thickness, from 0.691 mm for (0.5+0.5 mm) to 1.2385 mm for (0.5+0.9 mm). Rivet head height decreased from 0.2239 mm to 0.1301 mm with thicker sheets, while the minimum remaining material thickness increased, reaching 0.2614 mm in the (0.9+0.7 mm) configuration compared to only 0.021 mm in (0.5+0.5 mm). Higher interlock and thicker lower sheets improved load-bearing capacity in lap shear and T-peel tests, with the (0.9+0.9 mm) sheets showing the best performance. Joint success was strongly linked to the minimum remaining material thickness. Neural network analysis further demonstrated the potential to generate optimal die designs, reducing both cost and time.

**Keywords:** Self piercing rivet joint (SPR), Die geometry, Numerical Analysis, Neural Network, Joint interlock, Joint quality

### 1. Introduction

The joining of sheet metals is an important process in the automotive and aerospace industries. The manufacturers aim to use lightweight materials with high strength capacity in order to reduce cost and increase fuel consumption efficiency. Common welding processes such as spot welding are inappropriate for this purpose due to the differences in melting points and thermal conductivity [1]. To overcome these restrictions, new processes had been developed like clinching, friction stir welding, and self-piercing riveting (SPR). SPR is a high-speed sheet assembly, mechanical fastening method [2].

In this process, a rivet is used to penetrate the upper sheet by pressing the punch and then the tail rivet will spread in the lower sheet using a suitable die. The SPR process can join dissimilar materials, such as aluminum with plastics, also "hard-to-weld" materials, such as coated sheet metal. Compared with spot-welding, SPR can produce better joints in both "high-strength, low-alloy steel" and aluminum [3].

Gaining insight into the joint formation process during SPR is very challenging. The effective way to analyze SPR joints during the forming process is to perform numerical simulation. Over the past two decades, several researchers have investigated the SPR process both experimentally and numerically. For instance, Porcaro et al.



(2006) examined the effects of friction, mesh size, and die type on riveting force in aluminum alloys, highlighting the significant role of interfacial friction [4]. Qu and Deng (2008) modeled the influence of workpiece temperature, showing that higher temperatures substantially reduce the required punching force [5]. More recently, Li et al. (2013) and Shing-ling et al. (2014) studied the influence of rivet tip and die parameters on joint quality [6],[7]. These studies confirm that die geometry, sheet thickness, material properties, and friction conditions are among the most critical factors controlling joint performance.

Different finite element software was used such as MSC Super Form [5], LS-Dyna [8], DEFORM-2D [9, 7], and MSC Marc Mentat [10] to simulate the SPR process and study the effect of die geometry on material flow. The SPR process is affected by many parameters like sheet strength, sheet combination, and sheet temperature [11]. The process can be performed with different rivet materials like aluminum [6], or coated steel [12]. The die geometry and sheet thickness are the main SPR parameters that are studied to investigate their effects on this method. So, a series of experimental tests were implemented at variable die parameters and sheet thickness, then joint parameters (joint interlock, rivet head height, and minimum remaining material thickness) were measured on the self-pierced riveted joints.

The lap shear and T-peel are the experimental tests implemented to describe the influence of joint quality. The validity of the finite element model was calibrated and examined throughout the experiment's result of the riveting process. The material flow according to the die parameters was predicted by the calibrated finite element models which simulate the riveting process. Finally, the neural network approach was implemented by using the experimental and simulated results to clarify the effect of die geometry on joint structure.

Recent studies have highlighted significant benefits of integrating finite element modeling with machine learning techniques to optimize SPR processes, especially in addressing the complex interactions between die geometry and sheet thickness variation. For example, Wang et al. (2024) demonstrated that integrating experimental data with neural network models enhances the accuracy of joint performance predictions, emphasizing the importance of this study's approach in advancing SPR joint design and evaluation [13].

Although previous studies have addressed various aspects of the SPR process such as die geometry, sheet thickness, and material combinations, few have systematically combined experimental, numerical, and neural network approaches to analyze their combined effects on joint quality. In particular, the influence of asymmetric sheet thickness configurations on joint interlock and remaining material thickness remains underexplored.

## 1. Riveting Mechanism

The rivet material is forced into the punch cavity to create a mechanical bond between the sheets during the SPR process. The self-piercing riveting process consists of four basic steps, the sequence of which is as follows:

- 1) Primarily, settling the rivet above the sheets that are being joined,
- 2) Infiltrating the rivet for the upper sheet by punching press,
- 3) Upper sheet is sheared into two parts and then rivet infiltrates into lower sheet and the Infiltrating is beginning, and
- 4) Finally, Join is formed for both two sheets. [14] (See figure 1.)

The die design is the basic significance for processing efficiency and a quality production. The geometry of concave die is a direct impact on the joint structure for SPR joint. The design of a concave die includes many geometric parameters such as: the diameter of the concave die ( $d$ ), the lift height ( $h_r$ ), the cone radius ( $R$ ), the cone angle ( $\alpha$ ), the draft angle ( $\beta$ ), the fillet radii ( $r_1, r_2, r_3$ ) and the depth of the concave die ( $h$ ) [7]. Figure (3-12) illustrates the geometry of concave die. (see figure 2.)

The main schematic structure of the SPR joint is shown in Figure 3. Minimum remaining material thickness ( $t_m$ ), it is the vertical starch between the foot bottom of the rivet and the interface of the bottom sheet and die's cavity; determines the shear strength of the connection and the dynamic fatigue strength [6]. Interlock

( $\Delta x$ ), this distance determines the interface between sheet joints; it controls the joint tensile strength [15]. The rivet head height ( $t_h$ ) determines the depth of the rivet head penetration into the upper sheet and influences the mechanical quality of the joint [8].

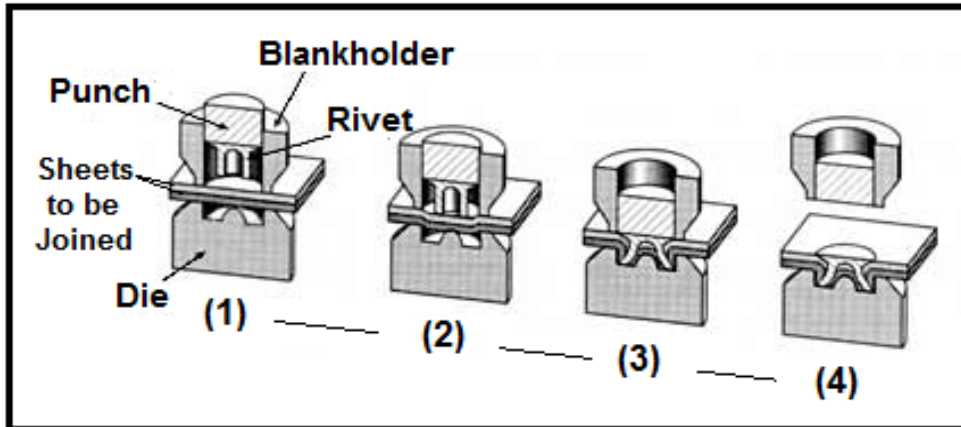


Figure 1. Self-Riveting Process Steps.

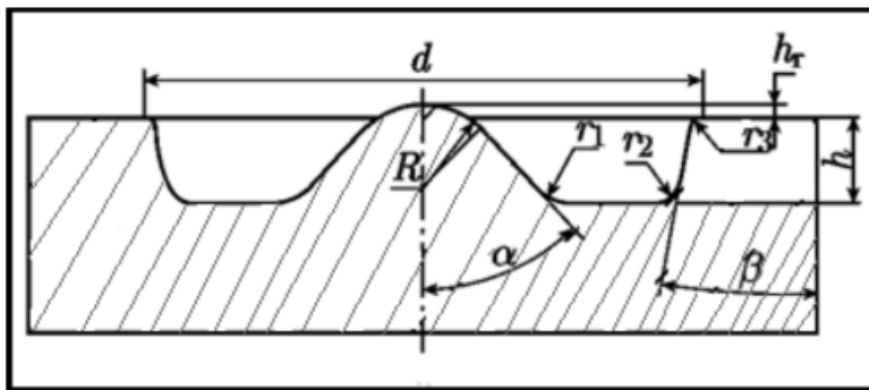


Figure 2. The concave dies parameters.

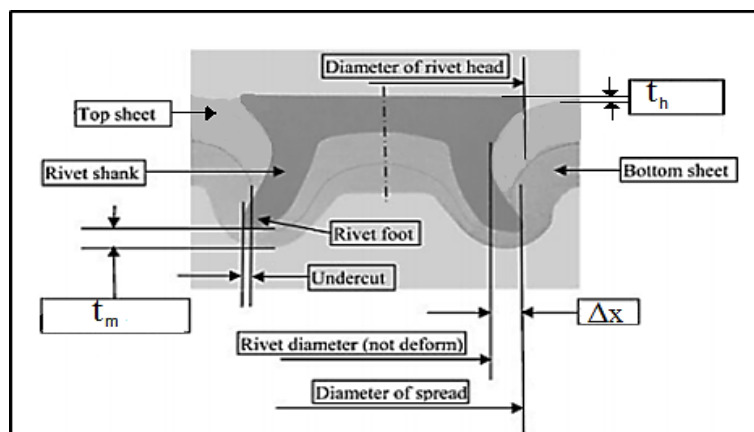


Figure 3. Schematic outline of the joint components.

## 2. Experimental procedure

### 2.1. Materials

Semi tubular AISI 1010 steel rivets (6mm diameter  $\times$  7mm length) were used to join AA 1060 sheets. The chemical composition of rivets and the sheet are listed in Tables (1) and (2). The strain hardening rule will be described in FE model. Then, the flow stress of the rivet and aluminum sheet was considered as ( $\sigma = k\varepsilon^n$ ), the values of (k and n) are shown in table (3).

Experimental sheets were cut to dimensions of (125×38 mm). Sheet thickness was used as a variable affecting the strength of the joint, so that three different sheet thicknesses were used (0.5, 0.7, and 0.9mm). CK45 Steel was used to manufacture concave die inserts. The die geometry contains many parameters as shown in figure 4. The die parameters are die depth (h), cone radius (R), and raised the height of the concave die (h<sub>r</sub>)

Table 1. Chemical composition of rivet AISI 1010 steel (wt. %)

C%	Si%	Mn%	P%	S%	Cr%	Ni%	Cu%	Fe%
0.102	0.035	0.297	0.024	0.005	0.028	0.005	0.043	99.46

Table 2. Chemical composition of 1060AL (wt. %)

Fe max%	Si max%	Mn max%	Mg max%	Cu max%	Zn max%	Ti max%	Other	AL min%
0.168	0.055	0.007	0.0001	0.005	0.011	0.012	0.02	99.7

Table 3. Mechanical properties of rivets and sheets

Material	Yield strength [MPa]	Tensile Strength [MPa]	Young Modules [GPa]	Poisson's Ratio	Flow stress
Steel1010	305	365	190	0.27	$\sigma = 229.376\varepsilon^{0.33}$
1060AL	56	112	69	0.33	$\sigma = 168.11\varepsilon^{0.134}$

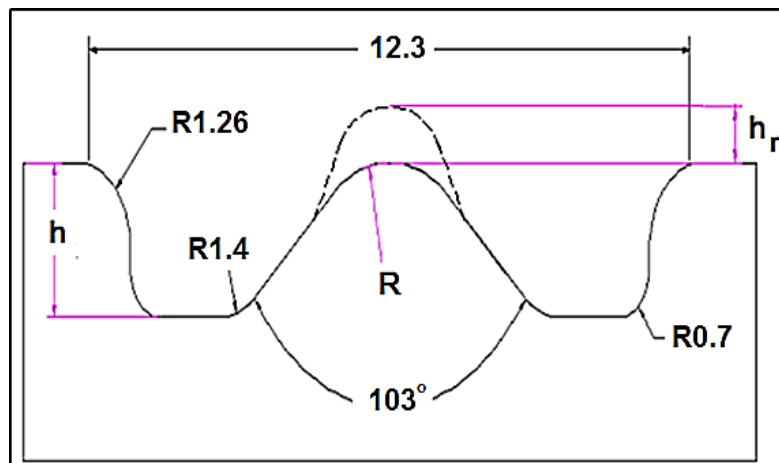


Figure 4. Geometry of concave die

We have four variables; each of them contains three values as listed in the table (4), so we have to perform ( $3^4 = 81$ ) tests. To reduce the number of tests, cost, and time, the orthogonal array test was adopted as shown in table (5).

Table 4. Variable parameters for die and sheet metal

Variables	Levels		
	First	Second	Third
<b>h</b>	<b>2.2</b>	<b>1.9</b>	<b>1.6</b>
<b>R</b>	<b>2.3</b>	<b>2</b>	<b>1.5</b>
<b>h<sub>r</sub></b>	<b>0</b>	<b>-0.3</b>	<b>0.2</b>
<b>t</b>	<b>0.5</b>	<b>0.7</b>	<b>0.9</b>

Table 5. Required tests according to the orthogonal array

Die No.	h	R	h <sub>r</sub>	t
1	2.2	2.3	0	0.5+0.5
2	2.2	2	-0.3	0.7+0.7
3	2.2	1.5	0.2	0.9+0.9
4	1.9	2.3	-0.3	0.9+0.9
5	1.9	2	0.2	0.5+0.5
6	1.9	1.5	0	0.7+0.7
7	1.6	2.3	0.2	0.7+0.7
8	1.6	2	0	0.9+0.9
9	1.6	1.5	-0.3	0.5+0.5

## 2.2. Pressing process

"Gunt WP 300 device" was used to perform the pressing process shown in figure 5. It is equipped with a dial gauge to measure the applied load during the riveting process. The rivet is attached to the moving part of the device while the die insert is located on the fixed part. The two plates to be jointed are placed between the rivet and the die insert. Constant load of (17kN) for all tests was applied to the rivet so that it penetrates the upper sheet and deforms within the lower sheet producing the required joint. For each die insert, the two configurations of jointed plate include lap-shear and T-peel sample were produced as shown in figure 6.

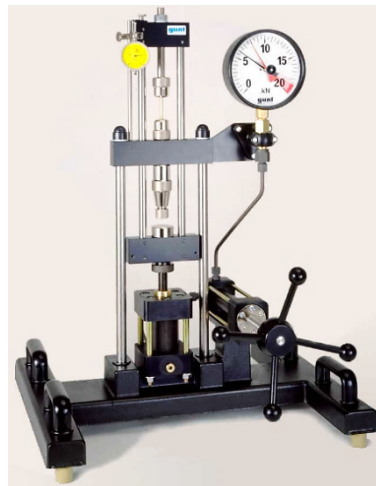


Figure 5. The Gunt WP 300 device

The strength of the SPR joint is obtained by the strength of the mechanical interlock mechanism between the rivet shank and sheets. To determine joint strength, Lap shear and T-peel samples were prepared as shown in figure 7.

To measure the required dimensions of the riveted joint samples, each sample was sectioned and polished with emery paper. The image of the section was inserted into AutoCAD software and scaled to the real dimensions of the joint. Lines were drawn at the places of interest and the distances between these lines were measured as shown in figure 8.

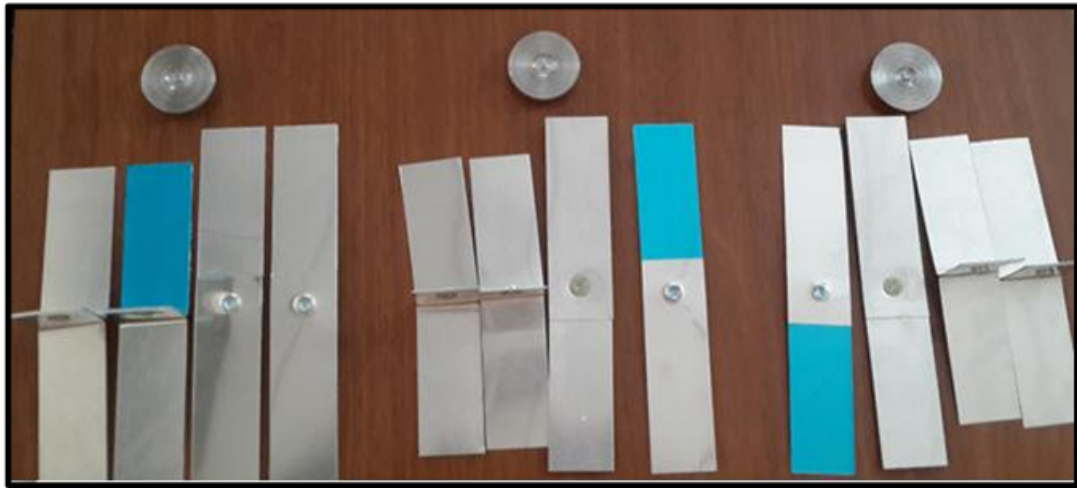


Figure 6. Jointed plate configurations

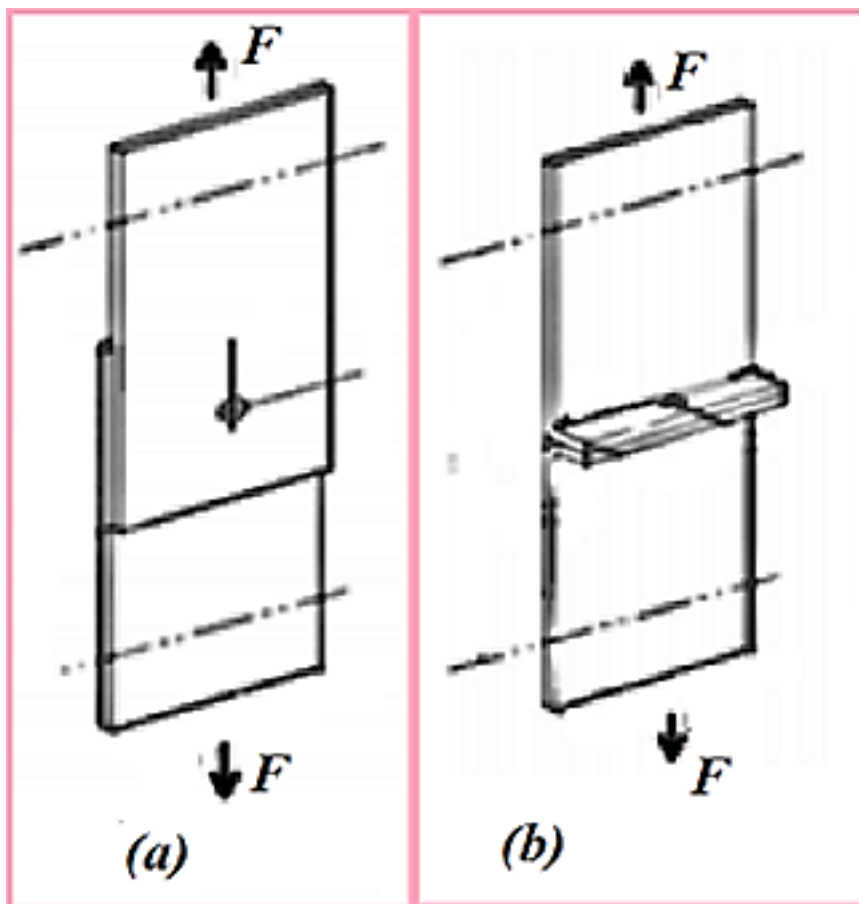


Figure 7. Joint strength test samples; (a) Lap shear and (b) T-peel.

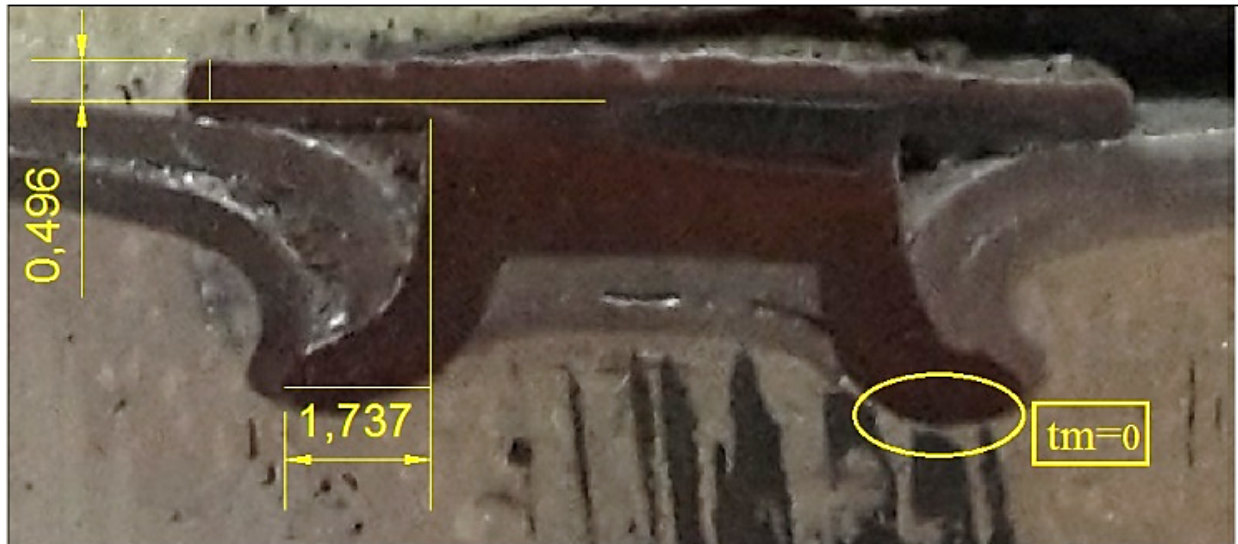


Figure 8. Image processing of joints

### 3.2 Modeling Approach

A model of the SPR process was developed using "Simufact Forming" FE software to predict the joint structure and material flow for different die parameters and sheet thickness. Different element lengths were tested, thus elements of the quad (10) type and lengths of 0.15mm and 0.03mm were assigned for plate and rivet respectively. To preserve the mesh from excessive distortion, quad tree remesher was involved. A hydraulic press was assumed at constant velocity of 20 mm/s, die spring stiffness (250 N/mm), friction parameters for all joints were chosen as combined Coulomb and Shear stress friction with coefficients of 0.1 and 0.2 respectively. Force of 17KN was applied in order to fit the process conditions. To validate the assumed numerical model, the model expectations at the same processing conditions were compared with experimental measurements. Finally, forward propagation neural network approach was implemented. The network consists of four nodes representing the input data of die profile parameters and plate thickness, three nodes representing target data of joint structure parameters, and one hidden layer composed of ten neurons as in figure 9.

## 4. Results and Discussion

### 4.1. Effect of Total Sheet Thickness on Joint Structure

Three sets of similar sheet thickness were used: (0.9+0.9) mm, (0.7+0.7) mm and (0.5+0.5) mm. Die parameters were ( $h=1.9$ ,  $R=2.3$ ,  $h_r=-0.3$ ) mm. It was found that increasing the sheet thickness increases the joint interlock as in figure 10; this is due to increase the rivet flaring in the sheets. The rivet head height decreases with increasing the total sheet thickness as shown in figure 11; this is due to increasing the penetration volume of the rivet. Decrement in rivet head height reduces gaps between rivet and upper sheet, which in turn produce better joints; similar observations were reported by Li et al. (2013), and this result is in agreement with that found by [15].

Increasing sheet thickness leads to increases the minimum remaining material thickness as in figure 12. When sheet thickness increases, the spreading of rivets increases too, and the crack occurrence is reduced. Finally, increasing plate thickness increases the joint interlock which in turn increases the maximum load required to disjoint the sheets as shown in figure 13.

The maximum load depends on the amount of joint interlock. Poor interlock leads to insufficient cohesion between the sheets, thereby reducing both the shear and T-peel forces. The lap-shear force was higher than the T-peel force because the lap-shear test primarily represents direct shearing of the rivet material, The T-peel load indicates the resistance of the joined sheets to bending through  $90^\circ$  without crack initiation or joint failure. An experimental investigation, supported by numerical simulation using Simufact Forming software, was carried out to examine the influence of die depth on the joint formation in self-piercing riveted aluminum sheets.

All other die parameters were kept constant to ensure that the observed variations were solely attributed to changes in die depth. The results revealed that increasing the die depth initially enhances the joint interlock by providing additional space for rivet leg expansion within the die cavity. This improvement in interlock contributes to better mechanical engagement between the joined sheets. However, when the die depth exceeds an optimal value, the rivet tends to penetrate deeper into the lower sheet rather than spreading laterally, leading to a reduction in interlock efficiency and overall joint quality.

Moreover, die depth exhibited an inverse relationship with rivet head height. As the die depth increased, the rivet head height decreased due to greater rivet penetration and deformation. Beyond the optimal depth, this trend reversed slightly because the reduced interlock limited the extent of rivet deformation, resulting in a marginal increase in head height.

This result is consistent with more recent investigations which reported that higher interlock values enhance lap-shear strength and reduce premature cracking [18, 19]. The numerical results are (98%) in agreement with the experimental results which indicates the validity of the numerical model.

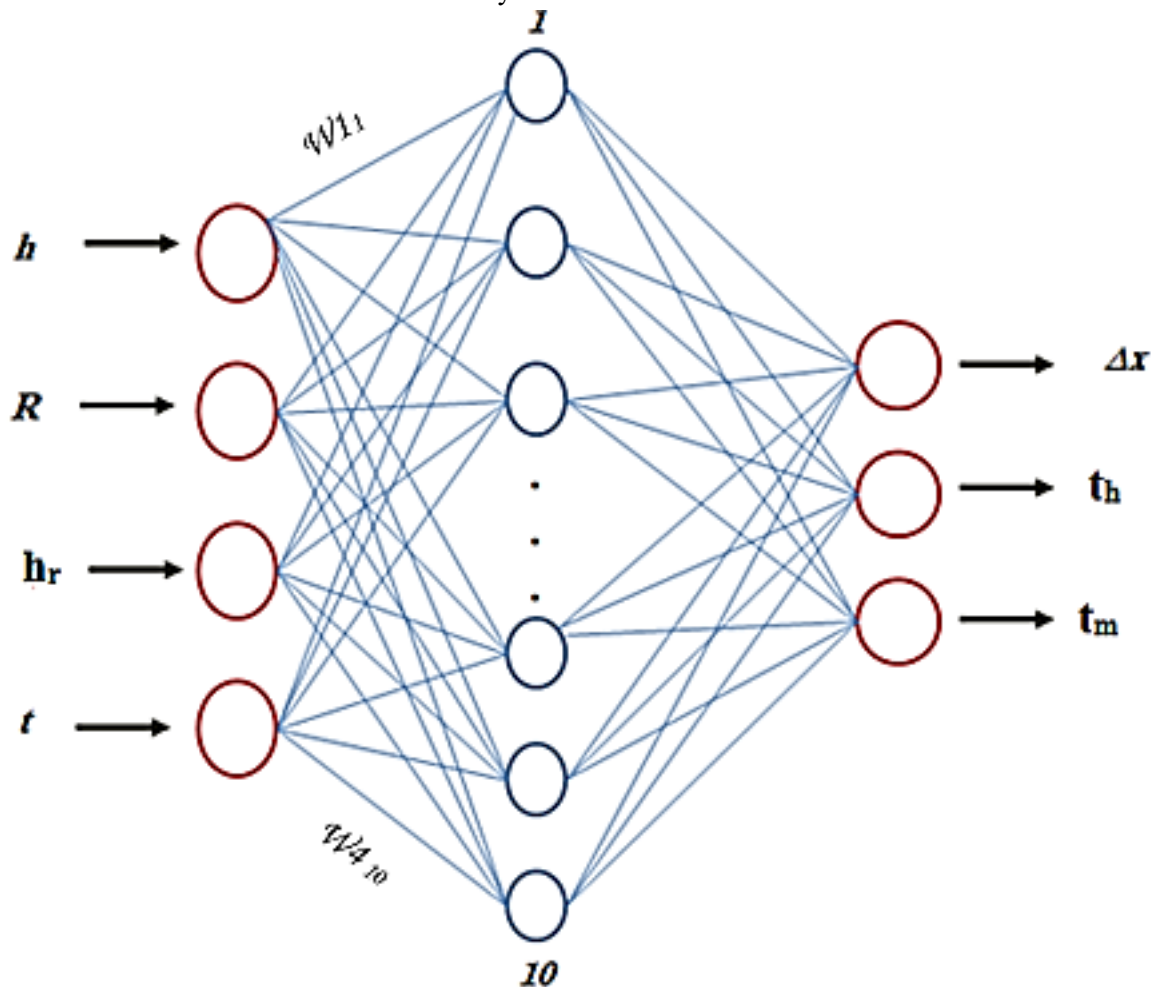


Figure 9. Proposed neural network

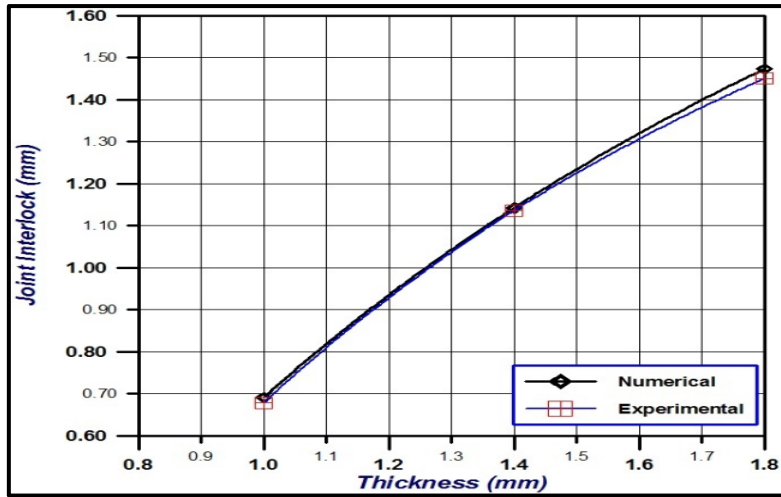


Figure10. Relationship between sheet thickness and joint interlock

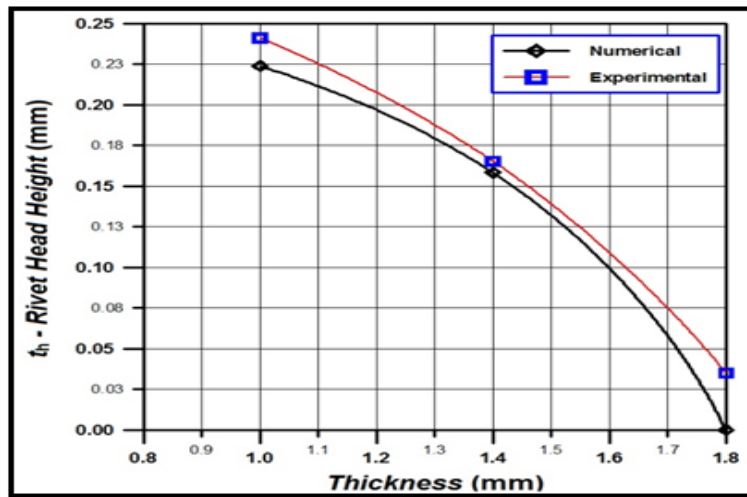


Figure11. Relationship between sheet thickness and rivet head height ( $t_h$ )

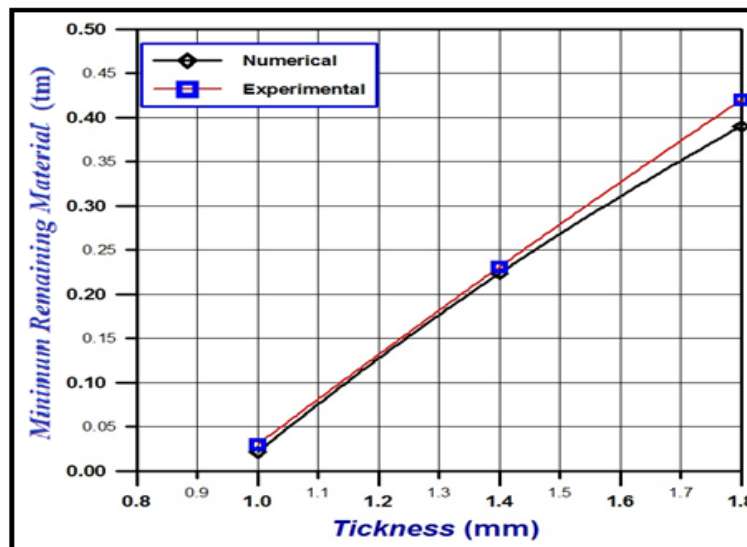


Figure12. Effect of sheet thickness on minimum remaining material thickness

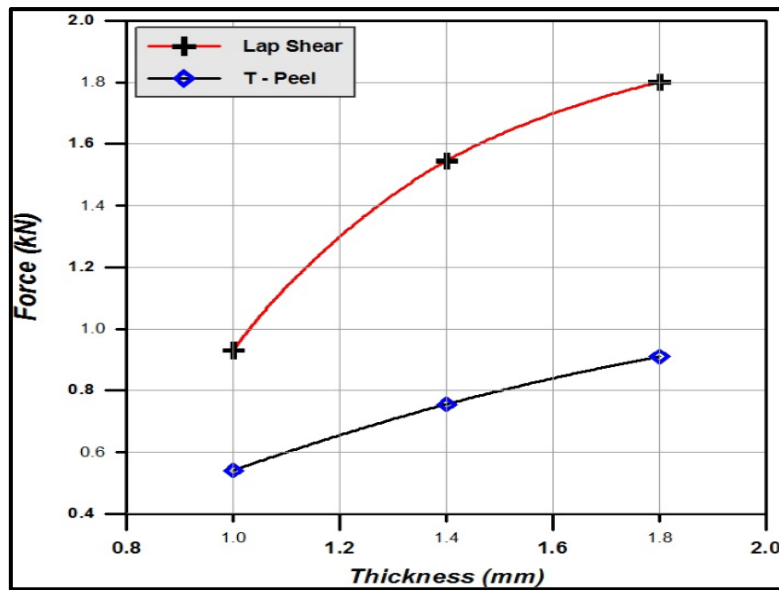


Figure13. Lap-shear and T-peel force variation with sheet thickness.

#### 4.2. Effect of plate thickness distribution in Joint Structure

Increasing the lower sheet thickness increases the joint interlock and the minimum remaining material thickness while decreasing the rivet head height as in table 6. As the lower sheet thickness increases, the work hardening in front of the rivet leg increases, which results in increasing the hardness locally and in turn increases the rivet flaring. Increasing upper sheet thickness decreases joint interlock and rivet head height while increasing the minimum remaining material thickness because the rivet starts flaring within the upper plate. In contrast, increasing the upper sheet thickness reduced the interlock and rivet head height but increased the minimum remaining material thickness, since the rivet tended to flare within the upper plate rather than penetrating deeper into the lower plate. This finding aligns with the work of Shing-ling et al. (2014) [7].

Table 6: joint structure results at different plate thickness distributions

Plate Thickness	Joint interlock $\Delta x$	Rivet head height (th)	Minimum remaining material thickness (tm)
0.5+0.5	0.691	0.2239	0.021
0.5+0.7	1.1456	0.1856	0.1241
0.5+0.9	1.2385	0.1301	0.15
0.7+0.7	1.1423	0.1584	0.2233
0.9+0.7	1.1242	0.1365	0.2614

#### 4.3. Neural Network Result

Nine experimental and fifteen numerical results were used as input parameters for the neural network with one hidden layer consisting of 10 nodes. Die parameters were considered as input data, while joint structure results were considered as target data. After training the network, the weight factors were obtained as shown in table (7). Finally, three dies were used to perform an experimental test. The parameters of these dies are shown in table (8). The network results were verified by experimental tests as shown in table (9). It is obvious that the predicted results are in high agreement with the experimental results which gives good validity of the neural network to obtain the remaining factors that affect the SPR process.

Table 7. Weight factors of the neural network

j	W1,j	W2,j	W3,j	W4,j
1	1.08940	-1.787000	1.213200	0.80274
2	0.82846	1.389500	-2.147400	-0.16359
3	-1.08600	1.37820	1.086100	-1.18380
4	1.31610	-0.098369	1.218900	-1.99730
5	1.15960	0.850560	-0.015766	-1.17410
6	0.15343	-1.707600	2.443800	1.68350
7	-0.81909	-1.049200	1.953800	1.15230
8	0.20084	1.801100	-0.541590	-0.76592
9	2.67150	-0.153930	1.126800	1.98670
10	1.40730	1.393700	0.145650	-0.78993

Table8. Extra dies parameters

Die No.	h	R	hr	t
10	2.2	1.5	0	0.5+0.5
11	1.9	2.3	-0.3	0.7+0.7
12	1.6	2	-0.3	0.9+0.9

Table 9. Experimental and neural prediction results

Die No.		$\Delta x$ (mm)	th(mm)	tm (mm)
<b>10</b>	Experimental	1.2334	0.2844	0.1355
	Predicted	1.2450	0.2895	0.1371
<b>11</b>	Experimental	1.1364	0.1584	0.2233
	Predicted	1.1359	0.1579	0.2160
<b>12</b>	Experimental	1.2653	0.3970	0.3704
	Predicted	1.2640	0.3850	0.3620

## 5. Conclusions

From the present work it can be concluded that:

1. The minimum remaining material thickness is a reliable visual indicator of joint quality; joints with zero remaining thickness are considered failed.
2. The upper and lower sheet thicknesses play a critical role in joint performance. Higher upper sheet thickness increases rivet deformation, while maintaining a thicker lower sheet improves interlock and prevents cracks.
3. Die depth significantly affects joint quality. Increasing depth up to 2.2 mm enhances interlock but reduces both minimum remaining material thickness and rivet head height.
4. Cone radius has opposite effects: larger radii increase remaining material thickness and rivet head height but decrease interlock.
5. The raised height should be aligned with or below the die surface to avoid failure.
6. Experimental results confirmed that the dominant failure mode in SPR joints under loading is shear failure, with joint strength efficiency considered the key factor in die profile optimization.
7. The numerical model accurately represented the SPR process with an average error of about 3%, and Neural Network analysis proved effective in generating optimized die designs with reduced cost and time

### Declaration of Competing Interest

The authors declare that there are no conflicts of interest regarding the publication of this manuscript.

### Funding Information

No funding was received from any financial organization to conduct this research

### Author Contributions

All authors proposed the research problem. In addition to author Doaa Fadhil, Haibat Lafta collected recent articles and organized them in simple shapes. Apart from the writer, gathered up-to-date articles and arranged them in straightforward formats Doaa Fadhil was discussed by the writers. The design, findings, and completed version of this work were all suggested by Haibat Lafta Gataa.

### Acknowledgments

The authors express their gratitude to Wasit University/ College of Engineering Mechanical Engineering department in Al kut-Waist-Iraq for supporting this study.

### Notation list

Abbreviations	Meaning
t	Plate thickness
$\Delta x$	Joint interlock
th	Rivet head height
tm	Minimum remaining material thickness
h	die depth
R	cone radius
$h_r$	raised the height of the concave die

### References

- [1] X. He, I. Pearson, and K. Young, "Self-pierce riveting for sheet materials: State of the art," *Journal of Materials Processing Technology*, vol. 199, pp. 27–36, 2008.
- [2] R. Porcaro, A. G. Hanssen, M. Langseth, and A. Aalberg, "Self-piercing riveting process: An experimental and numerical investigation," *Journal of Materials Processing Technology*, vol. 171, no. 1, pp. 10–20, 2006.
- [3] P. O. Bouchard, T. Laurent, and L. Tollier, "Numerical modeling of self-pierce riveting—from riveting process modeling down to structural analysis," *Journal of Materials Processing Technology*, vol. 202, pp. 290–300, 2008.
- [4] L. Han, M. Thornton, and M. Shergold, "A comparison of the mechanical behavior of self-piercing riveted and resistance spot welded aluminum sheets for the automotive industry," *Materials and Design*, vol. 31, no. 3, pp. 1457–1467, 2010.
- [5] D. Li, L. Han, M. Shergold, M. Thornton, and G. Williams, "Influence of rivet tip geometry on the joint quality and mechanical strengths of self-piercing riveted aluminum joints," *Materials Science Forum*, vol. 765, pp. 746–750, 2013.
- [6] N.-H. Hoang, R. Porcaro, M. Langseth, and A.-G. Hanssen, "Self-piercing riveting connections using aluminum rivet," *International Journal of Solids and Structures*, vol. 47, pp. 427–439, 2010.
- [7] J. Mucha, "A study of quality parameters and behavior of self-piercing riveted aluminum sheets with different joining conditions," *Strojniški Vestnik – Journal of Mechanical Engineering*, vol. 57, no. 4, pp. 323–333, 2011.
- [8] Y. Abe, T. Kato, and K. Mori, "Self-pierce riveting of three high strength steel and aluminum alloy sheets," *International Journal of Material Forming*, vol. 1, no. 1, pp. 1271–1274, 2008.

- 
- [9] H. Shan-ling, L. Zhi-yong, G. Yuan, and Z. Qing-liang, "Numerical study on die design parameters of self-pierce riveting process based on orthogonal test," *Journal of Shanghai Jiaotong University (Science)*, vol. 19, no. 3, pp. 308–312, 2014.
- [10] Y. Xu, "Effects of factors on physical attributes of self-piercing riveted joints," *Science and Technology of Welding and Joining*, vol. 11, no. 6, pp. 666–671, 2006.
- [11] E. Kaščák, "Joining materials by self-piercing riveting method," *Transfer Inovácií*, no. 22, pp. 43–46, 2012.
- [12] J. Wang, L. Zhang, M. Li, and S. Chen, "Integration of finite element simulation and neural network modeling for optimizing die geometry and sheet thickness in self-piercing riveting," *Journal of Manufacturing Processes*, vol. 75, pp. 123–135, Apr. 2024.
- [13] S. G. Qu and W. J. Deng, "Finite element simulation of the self-piercing riveting process," in *Proceedings of the International Mechanical Engineering Congress and Exposition (IMECE)*, Boston, MA, USA, Oct. 31–Nov. 6, 2008, pp. 1–6.
- [14] D. Li, A. Chrysanthou, I. Patel, and G. Williams, "Self-piercing riveting – a review," Working Paper, University of Warwick, Coventry, UK, 2016. [Online]. Available: <http://wrap.warwick.ac.uk/79605> Theses and Dissertations
- [15] S. J. Durbin, *Friction-Stir Riveting: An Innovative Process for Joining Difficult-to-Weld Materials*, M.S. thesis, Dept. Mechanical, Industrial & Manufacturing Engineering, University of Toledo, Ohio, USA, 2012.
- [16] P. H. Holmstrøm and J. K. Sønstabø, *Behavior and Modeling of Self-Piercing Screw and Self-Piercing Rivet Connections*, M.S. thesis, Dept. of Structural Engineering, Faculty of Engineering Science and Technology, NTNU, Trondheim, Norway, 2013.
- [17] J. Ioannou, *Mechanical Behavior and Corrosion of Interstitial-Free Steel to Aluminum Alloy Self-Piercing Riveted Joints*, Ph.D. thesis, School of Engineering and Technology, University of Hertfordshire, England, UK, 2009.
- [18] P. J. Johnson, *Online Monitoring of Self-Pierce Riveting Systems to Provide Non-Destructive Testing of the Mechanical Interlock*, Ph.D. dissertation, Liverpool John Moores University, UK, 2013.
- [19] L. Han, *Mechanical Behavior of Self-Piercing Riveted Aluminum Joints*, Ph.D. dissertation, University of Hertfordshire, in collaboration with Alcan International Ltd. and Textron Fastening Systems, 2003.